A building integrated solar air heating thermal collector prototype: modelling, validation and case studies

A. Buonomano[a], C. Esposito[a], S.A. Kalogirou[b], A. Mosphiliotis[b], A. Palombo[a*], Z. Symeou[b]

[a] *Department of Industrial Engineering, University of Naples Federico II, P.le Tecchio, 80, 80125 Naples, Italy*

[b] *Department of Mechanical Engineering and Materials Science and Engineering, Cyprus University of Technology - P.O. Box. 50329, 3603 Limassol. Cyprus*

Abstract

In this paper, the energy performance simulation model of a new Flat-Plate Solar Thermal Collector (FPC) prototype with air as working fluid, is presented. The collector is designed to be integrated in the building envelope. With respect to existing commercial collectors such prototype is characterized by lower initial costs. The developed model is implemented in a computer code written in MatLab for the whole building energy, economic and environmental performance analysis. Specifically, the presented model is able to predict both the active and passive effects of the building integrated solar collector. The collector simulation model was validated by means of suitable experimental data collected at Limassol (Cyprus).
In order to show the features of the developed simulation code, a comprehensive case study was developed. Here, the performances of both traditional stand-alone and building integrated collectors are analysed. In particular, the examined prototype is modelled as integrated on a South building façade of a multi-floor commercial building, located in different weather zones. Simulation results show that interesting energy saving can be achieved vs. traditional reference buildings, especially in cold winter climates and high heating demands.

1. Introduction

The main goal of solar collectors is to produce as much thermal energy as possible at the minimum total cost. To this aim, particular attention is paid to design novel concepts which may increase the collection of solar energy and boost the building integration. Among the available typologies of solar panels, stationary Flat Plate Collectors (FPCs), are one of the most cheaper technology to be manufactured and installed. Through FPCs, the absorbed solar energy is exploited for different purposes through a suitable working fluid (Kalogirou 2014). In order to reduce conduction thermal losses, the back plate and frame of the collector are well insulated. In addition, a simple and/or low-e glass cover is often adopted in order to reduce convective and radiative heat losses. The heat transferred to the working fluid is enhanced by a suitable collector absorber plate.
In this paper a novel solar collector prototype with air as working fluid suitable to be integrated in building façades is presented. For such device a new dynamic simulation model was developed. In order to assess both the solar collector passive and active effects, the developed model was embedded in another simulation tool for the whole building energy, economic and environmental analysis. The complete dynamic simulation model was implemented in a computer code written in MatLab. In order to show the potentiality of such code a suitable case study was developed. In particular, it refers to a non-residential building equipped by the examined integrated solar collectors. Simulations are carried out for different climate conditions. Useful results are achieved for both building designers and solar collectors manufacturers.

2. Solar collector prototype

The prototype solar collector is designed with the aim to boost the heat exchange, through a multi-pass serpentine configuration, as shown in Fig. 1. This system layout aims at counteracting and overcoming the intrinsic air collectors drawback, such as the low heat transfer between air and absorber plate. A low-e iron glass cover was adopted to reduce the

* Reference author email address: adolfo.palombo@unina.it

solar collector thermal losses (a very low transmittance for long wave thermal radiations is obtained). In order to obtain a lightweight, low cost and good efficiency device, the 8 prototype air channels and the back plate are designed by using aluminium sheets. The absorber plate is made by a thin iron plate (0.6 mm thickness), painted by high absorptance black varnish. With the aim to enhance the system thermal insulation, a wooden collector frame with an internal stone wool layer is adopted. In Table 1 the main design features of the building integrated solar collector prototype are summarised (here, l., w., h., d and th. represent length, width, height, distance and thickness, respectively).

Fig. 1. Air collector prototype: internal configuration and exterior design

Table 1. Features of the experimental setup

Collector l. [mm]	1631	Glass ε [-]	0.95
Collector w. [mm]	846	Insulation, k [W/mK]	0.03
Glass-abs d. [mm]	50	Edge, k [W/mK]	0.12
Insulation th. [mm]	50	Absorber, ε [-]	0.90
Duct w. [mm]	105	Glass/absorber, τα [-]	0.85
Duct h. [mm]	75	Back plate, ε [-]	0.90
Metal sheet th. [mm]	0.8	Brick th. [mm]	250
Number of ducts [-]	8	Brick, k [W/mK]	0.36
Absorber th. [mm]	0.6	Edge th. [mm]	50

2.1. Solar collector simulation model

For the energy performance assessment of the collector, a suitable dynamic model implemented in a computer simulation code, is developed. The mathematical model is derived by those proposed by (Duffie and Beckman 2013) and (Kalogirou 2014). The main assumptions in the related energy algorithms are: thermodynamic equilibrium; steady state regime; one dimensional heat transfer; negligible kinetic and gravitational terms; negligible temperature gradients around ducts or pipes; homogeneous, isotropic and time independent properties of materials; uniformly concentrated radiation on the absorber; no solar energy absorbed by the glass cover; negligible temperature drop through the cover; negligible dust effects on the cover; same boundary ambient temperature on front and back of the collector face; no shadings on the absorber plate.

2.1.1. Energy losses

The convection, conduction and radiation heat losses occurring in the solar collector can be schematized through the thermal network sketch of Fig. 2.

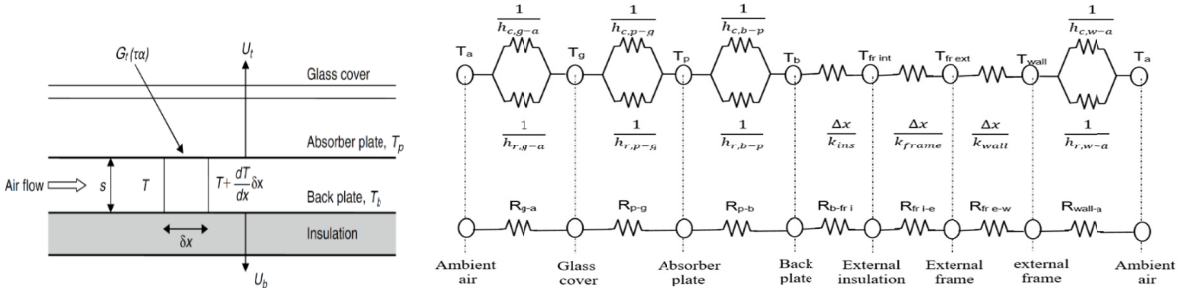

Fig. 2. Air solar collector scheme and related thermal network

where: T_p, T_a and T_g are the absorbing plate, ambient air and glass cover temperatures [K], respectively. R [K/W] are the thermal resistances. The energy losses can be estimated by:

$$Q_{loss} = \frac{T_p - T_a}{R_L} = U_L A_C \left(T_p - T_a\right) \qquad \text{Eq. (1)}$$

where: R_L [K/W] is the combined thermal resistance and U_L is the overall (bottom and edges) heat loss coefficient [W/m^{2}K] based on collector area A_C. In a well-insulated collector, the main heat losses are those through the top of the device. In case of a single glass cover, the heat loss from the front of the collector acts in two different ways: i) from the absorber plate to the glass cover; ii) from the glass cover to the ambient air. The first can be calculated as:

$$Q_{t,a-g} = A_C h_{c,p-g}\left(T_p - T_g\right) + \frac{A_C \sigma\left(T_p^4 - T_g^4\right)}{\frac{1}{\varepsilon_p} + \frac{1}{\varepsilon_g} - 1} \qquad \text{Eq. (2)}$$

where $h_{c,p-g}$ is the convection heat transfer coefficient between the absorber plate and glass cover [W/m^{2}K]; σ is the Stefan-Boltzmann constant, ε_p and ε_g are the absorber plate and glass cover emissivity. Similarly, the heat loss from the glass to the ambient can be calculated as:

$$Q_{t,g-a} = A_C\left(h_{c,g-a} + h_{r,g-a}\right)\left(T_g - T_a\right) \qquad \text{Eq. (3)}$$

where $h_{c,g-a}$ is the convective heat coefficient between the glass and the air and $h_{r,g-a}$ is the radiative one. Finally, the energy losses from the top of the solar collector to the ambient air are calculated as:

$$Q_t = \frac{\left(T_p - T_a\right)}{R_t} = U_t A_C\left(T_p - T_a\right) \qquad \text{Eq. (4)}$$

where R_t is the overall top resistance.

2.1.2. Energy and outlet air temperature assessment

Under steady-state conditions the rate of useful heat delivered by a solar collector to the working fluid is equal to the rate of energy absorbed by the heat transfer fluid minus the heat losses from the surface to the surroundings:

$$Q_u = A_C\left[G_t\left(\tau\alpha\right) - U_L\left(T_p - T_a\right)\right] = \dot{m} c_p\left(T_o - T_i\right) \qquad \text{Eq. (5)}$$

where: G_t is the incident total solar radiation, $\dot{m}$ is the air mass flow rate [kg/s], T_o and T_i are the air outlet and inlet temperatures. It worth noting that $(\tau\alpha)$ takes into account the multiple reflections of the solar radiation within the air gap between the absorber plate and the glass cover. A general formulation for the calculation of the solar thermal collector efficiency can be obtained from the Hottel-Whillier equation (Duffie and Beckman 2013). Here, in order to calculate the fluid outlet temperature (T_o) an iterative procedure is necessary. To simplify the procedure, it is possible to consider the useful heat as a function of the inlet temperature (T_i) by taking into account the so-called heat removal factor (F_R). Thus, the useful energy can be calculated as:

$$Q_u = A_C F_R\left[G_t\left(\tau\alpha\right) - U_L\left(T_i - T_a\right)\right] \qquad \text{Eq. (6)}$$

where the heat removal factor (F_R) represents the ratio of the actual energy gain to the useful energy gain of a collector, calculated as if the whole collector absorbing surface is at the fluid inlet temperature. At last, once F_R is calculated, the solar collector efficiency ($\eta = Q_u/A_c G_t$) can be rewritten as:

$$\eta = F_R\left[\left(\tau\alpha\right) - \frac{U_L\left(T_i - T_a\right)}{G_t}\right] \qquad \text{Eq. (7)}$$

By analysing the scheme of the air heating collector in Fig. 2 the air temperature distribution

inside the collector can be obtained through several energy balances. The outlet air temperature can be obtained as:

$$T_o = T_i + \frac{1}{U_L}\left[G_t(\tau\alpha) - U_L(T_i - T_a)\right]\left[1 - \exp\left(-\frac{A_C U_L F'}{\dot{m} c_p}\right)\right] \qquad \text{Eq. (8)}$$

More details are available in (Kalogirou 2014).

2.1.3. Model validation

To prove the reliability of the developed solar collector dynamic simulation model, an experimental validation procedure is performed. The experimental results were obtained through several tests carried out at Archimedes Solar Energy Laboratory (ASEL), Cyprus University of Technology, Limassol (Cyprus). The experimental setup was installed outside (Fig. 1) and the measurements were performed on three sunny days (April 7th, 18th and 27th 2016). The following parameters were investigated: i) G_t, global radiation on the vertical surface; ii) T_a, outdoor air temperature; iii) w, wind velocity; iv) $\dot{m}$, air mass flow rate; v) T_G, glass temperature; vi) T_{P1}, absorber plate temperature at the inlet section; vii) T_{P2}, absorber plate temperature at the outlet section; viii) T_o, outlet air flow rate temperature. The adopted thermocouples (K type; resolution: 0.1°C; accuracy 0.5% ±1°C) were connected to a suitable digital thermometer (Tecpel DTM-318). The air mass flow rate was measured by means of a hot wire anemometer (Omega HHF2005HW; measuring range: 0.2 to 20 m/s and 0 to 50°C; resolution: 0.1 m/s and 0.1°C; full scale accuracy: ±10 %+lsd and ±0.8°C). The air was circulated within the collector by means of a suitable fan (Soler & Palau TD 160/100) with a flow rate of 0.16 m^3/s. The solar radiation incident on the collector was measured through a pyranometer. The related output (mV) was accounted by a multimeter (Mastech MS82; measuring range: 0 to 320 mV; resolution: 0.1 mV; accuracy: ±0.7%). The measured data adopted as input in the developed model were: G, T_a (i.e. equal to the inlet air temperature), w, $\dot{m}$. For the validation procedure, simulation results of T_P, T_G, T_o and η were compared to the measured ones (note that, T_P was accounted as the average one of the two measured temperatures T_{P1} and T_{P2}). In Fig. 3 the simulation and experimental results are reported for only one sample day (April 18th 2016, from 10:30 to 17:00).

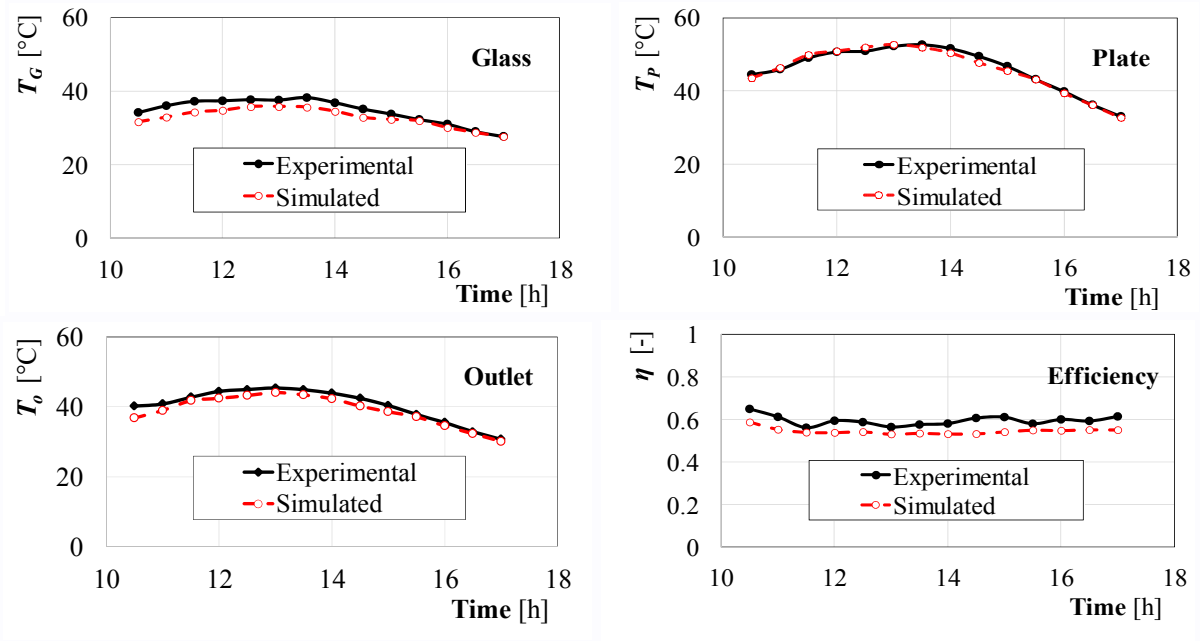

Fig. 3. Comparison of experimental and simulated results

As it is possible to observe, the developed simulation model shows a good reliability (a good agreement between simulated results and collected experimental data is detected). A similar correspondence is also obtained for the other two days in which the measurements were performed (April 7th and 28th, 2016). For all the test days, the average percentage differences ($\Delta_{m\%}$) between predicted and measured T_G, T_P, T_o, and η are reported in Table 2. Note that, such differences result always lower than 6.4% for T_G, T_P and T_o and lower than 13.4% for η. At last, the obtained average efficiency of the solar collector resulted 58%.

Table 2. Average percentage differences between simulated and experimental results

Test day	*April 7th*				*April 18th*				*April 27th*			
Parameters	T_G	T_P	T_o	η	T_G	T_P	T_o	η	T_G	T_P	T_o	η
$\Delta_{m\%}$ [%]	1.7	2.1	6.4	13.4	5.1	1.5	3.7	8.2	3.5	4.9	3.0	8.9

3. Building energy analysis: model and validation

As it is well known the building energy behaviour is influenced by the solar collectors integrated into the envelope (passive effect). Therefore, in order to carry out a complete energy, economic and environmental analysis a complete simplified dynamic simulation tool was developed and validated. The whole building-collector system was modelled through a suitable thermal network taking into account building elements layers, indoor and outdoor air temperatures and internal and external thermal loads. The thermal network is solved through the finite difference method where in each *t*-th time step and for each *n*-th node of the *m*-th building element the following energy balance equation is taken into account:

$$C_{m,n}\frac{\Delta T_{m,n}}{\Delta t}\sum_{j,n-1}^{n+1}\frac{T_{(m,j)}-T_{(m,n)}}{R_{m,j-n}^{cond}}=\dot{Q}_{m,n} \qquad \text{Eq. (9)}$$

where t is the time, $C_{m,n}$ and $T_{m,n}$ represent the thermal capacitance and the temperature of the n-th node of the m-th building element, respectively. $T_{m,j}$ is the temperature of the neighbour (n-1)-th and (n+1)-th nodes directly connected to the n-th one. $R_{m,j-n}^{cond}$ is the sum of the halves sub-layers thermal resistances that link the n-th node to their neighbour ones. Such total resistance is equal to the one of half sub-layer when the $n=1$ and $n=N$ capacitive nodes are linked to the surface non-capacitive ones. $\dot{Q}_{m,n}$ represents the generic thermal source term acting on the system node. The HVAC system is activated when the indoor air temperature is out of the comfort temperature range. More details are available in (Buonomano and Palombo 2014). Together with the solar collector model such equations are implemented in a suitable computer tool written in MatLab. Here, the building heating and cooling demands are calculated according to the selected HVAC system schedules and indoor air temperature set points. The presented model was validated by adopting the prEn 15625 standard procedure (residential use in the weather zone of Trappes, France). The validation procedure consists of eight different cases (from 5 to 12, taking into account different envelope layers layouts and internal gains) (PrEn15625 2007). The simulated heating and cooling demands ($Q_{H,pred}$ and $Q_{C,pred}$) are compared vs. the standard reference ones ($Q_{H,ref}$ and $Q_{C,ref}$). The results are reported in Table 3. In prEn 15625 the accuracy level of the proposed simulation model is detected by: $r_{QH} = |(Q_{H,pred}-Q_{H,ref})|/(Q_{H,ref}+Q_{C,ref})$ and $r_{QC} = |(Q_{C,pred}-Q_{C,ref})|/(Q_{H,ref}+Q_{C,ref})$. Three levels of accuracy are set by such validation procedure: Level A ($r_{QH,}$ $r_{QC} \leq 0,05$); Level B ($r_{QH,}$ $r_{QC} \leq 0,10$); Level C ($r_{QH,}$ $r_{QC} \leq 0,15$). Therefore, A or B levels are almost always achieved by the presented simplified simulation model. Note that a good agreement was also reached by comparing the simulation results vs. those obtained by TRNSYS and EnergyPlus.

Table 3. Model Validation by prEn 15625

Test n.	5	6	7	8	9	10	11	12
$Q_{H,ref}$ [kWh/m^{2}y]	23.4	25.7	53.9	15.8	37.7	29.0	70.4	26.9
$Q_{H,pred}$ [kWh/m^{2}y]	25.0	26.4	57.7	16.2	37.6	37.4	69.6	26.0
r_{QH} [%]	6.78	2.00	6.89	0.48	0.33	22.7	1.26	1.20
$Q_{C,ref}$ [kWh/m^{2}y]	10.2	9.35	0.99	57.2	7.99	9.72	0.71	46.9
$Q_{C,pred}$ [kWh/m^{2}y]	11.4	10.4	0.89	62.8	10.2	10.0	1.41	52.8
r_{QC} [%]	5.40	3.11	0.18	7.66	4.78	0.81	0.98	7.99

4. Case study

In order to show the potentiality of the developed dynamic simulation code a suitable case study is presented. It refers to a non-residential building consisting of a sample single thermal zone in a multi-floor building (middle grey coloured floor in Fig. 4). Floor and ceiling are considered as adiabatic whereas their capacitances and internal radiative heat exchanges are taken into account. The simulation assumptions, the main building features and the details of the building components are summarised in Table 4 and Table 5.

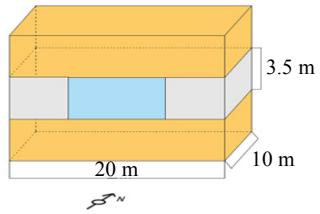

Fig. 4. Case study building

Table 4. Building features

Parameter	Value	Parameter	Value
Surface to Volume Ratio [%]	0.53	Wall absorptance, α	0.60
Floor Area [m^2]	200	Glazed surface area [m^2]	31.5
Volume [m^3]	700	Opaque South-wall area [m^2]	38.5
Heating/cooling set point [°C]	20/26	Window to wall ratio	45%
Occupancy [person/m^2]	0.06	Air infiltration [Vol/h]	1.0
South/North facing wall area [m^2]	70	Internal heat gains [W/m^2]	18
East/West facing wall area [m^2]	35	HVAC system schedule [h]	8-18

Table 5. Building layering layouts

Building component	Material	Thickness [mm]	c_p [J/kg K]	k [W/mK]	ρ [kg/m^3]
External Wall	Plasterboard	10.0	840	0.160	950
	Concrete block	200	860	0.680	600
	Plasterboard	10.0	840	0.160	950

The energy demand calculation was performed by considering the building with and without the integrated collectors. Different European weather zones are simulated in the carried out analysis through Meteonorm hourly weather files: Dublin, Copenhagen Freiburg, Naples, Limassol, Athens (sorted for increasing Incident Solar Radiation, ISR). In all the cases the above described solar collector prototypes are modelled as integrated only on the South building façade. All the available opaque surface is covered by 26 collectors (a parallel air circuit layout is taken into account with a total flow rate of 0.41 m^3/s, no thermal insulation is modelled between collectors and façade wall). A reference traditional building (without solar collectors and similar to the above mentioned one) was also modelled for comparison purposes. For both innovative and traditional buildings the heating and cooling is provided by an electric air-to-air heat pump/chiller (COP: 3). In the economic analysis an average electricity unitary cost of 0.18 €/kWh was considered for all the investigated Countries.

5. Results and discussion

For the developed case study both the solar collectors passive and active effects were assessed through the presented tool. Regarding the passive effects the results of the carried out analysis are shown in Table 6. Here, $Q_{H,trad}$ ($Q_{C,trad}$) and Q_H (Q_C) are the heating (cooling) demands of the traditional and innovative building, respectively. The building integration of the solar

collectors, in all the weather zones, leads to winter heating demand reductions (ΔQ_H) and to summer cooling requirement increases (ΔQ_C), as expected. In general, the calculated free heating effects appear weaker than the overheating ones. The latter results relevant in Limassol, Athens and Naples.

Table 6. Collector passive effects on the building energy demands [kWh/m^{2}y]

Weather zone	Dublin	Copenhagen	Freiburg	Naples	Athens	Limassol
$Q_{H,trad}$	61.9	82.14	68.6	23.7	16.0	9.81
Q_H	60.7	81.30	67.9	23.2	15.8	9.65
ΔQ_H	-1.20	-0.84	-0.69	-0.45	-0.30	-0.16
$Q_{C,trad}$	2.09	6.02	13.0	37.7	53.7	62.3
Q_C	2.50	6.65	14.4	40.2	55.9	65.6
ΔQ_C	0.41	0.63	1.40	2.54	2.23	3.29

In this case study the active effects take into account the energy saving achieved on the space heating demand through the solar thermal collectors (a direct free heating effect is obtained by directly supplying the outlet heated collector air to the building space). In Fig. 5 the calculated yearly thermal energies produced through a single collector (Q_{prod}) are reported. Higher productions are achieved in the investigated South-Europe zones (higher ISRs), as expected.

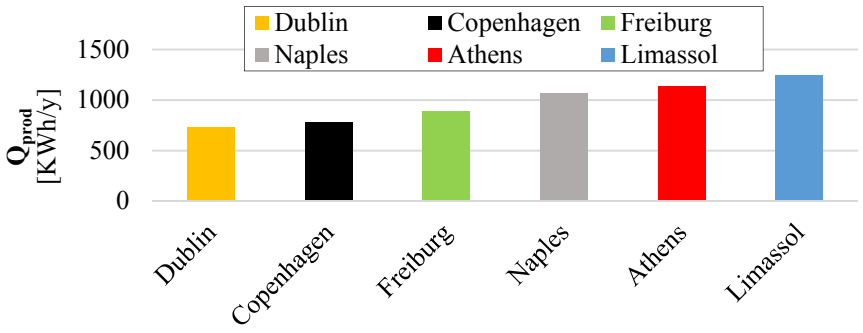

Fig. 5. Produced thermal energy through the solar collectors

Nevertheless, the proposed system layout is competitive also for applications in northern zones because of the modelled vertical layout of the solar panels (the vertical layout of the collectors is not so far from the optimal slope for the latitudes of the simulated locations, (Kalogirou 2014)). It is noteworthy to observe that not all the energy amount produced by the collectors is necessary to the building heating (in fact for the modelled air solar collectors system a heating supply/demand simultaneity is required since no heat storage system is taken into account). On the other hand, not all the heating needs can be fulfilled by the solar collectors (as expected in many winter times a heating integration is necessary through the auxiliary electric heat pump).

By the presented simulation tool it is possible to calculate for each selected time interval (specific hours, days, weeks, whole year, etc.) the rate of the building heating demand balanced by the solar energy. The results of this analysis are reported in Table 7 for the simulated building with 26 parallel integrated solar thermal collectors. Here, for the innovative system the yearly heat produced by the collectors and exploited for space heating (Q_u) as well as the related heating demands (Q_H) are reported. Note that, remarkable heating energy savings are achieved in all the investigated weather zones. In particular, where high solar radiations are reached high percentage heating demand ratios ($Q_{H,ratio} = Q_u/Q_H$) are obtained. In the same table the yearly savings (ΔE_{el}) of electricity consumption due to the heat pump/chiller vs. that one of the reference traditional building (without solar collectors) are also reported. Note that, such results take into account both the active and passive effects of

the building integrated solar thermal collectors. In Table 7 the yearly economic savings obtained vs. the traditional building are reported too. At last, by considering the national CO_2 emission factors linked to the electricity production (CO_2 factor) the yearly avoided CO_2 emissions are assessed. Obviously, the highest electricity, economic and emissions savings are obtained in the colder winter weather zones because of their higher heating needs, corresponding demands simultaneity with the collector thermal energy production and lower cooling requirements (the calculated savings for Dublin, Copenhagen and Freiburg surpass 28%).

Table 7. Energy, economic and environmental analysis

Weather zone	ISR [kWh/m^{2}y]	Q_u [kWh/y]	Q_H [kWh/y]	$Q_{H,ratio}$ [%]	ΔE_{el} [kWh$_e$/y]	[%]	Saving [€/y]	CO_2 factor [kg$_{CO_2}$/kWh$_e$]	ΔCO_2 [kg$_{CO_2}$/y]
Dublin	948	3752	12138	30.9	1304	30.5	235	0.73	954
Copenhagen	988	5040	16259	31.0	1694	28.8	304	0.46	781
Freiburg	1114	4724	13590	34.8	1527	28.0	275	0.62	953
Naples	1529	2324	4646	50.0	635	15.5	114	0.48	307
Athens	1561	1424	3152	45.2	346	7.44	62	1.15	398
Limassol	1843	1512	1930	78.4	296	5.89	53	0.87	258

6. Conclusions

In this paper a dynamic energy performance simulation model for a new flat plate solar thermal collector prototype with air as working fluid was developed and experimentally validated. The novelty of such solar panel consists in its simplicity and low initial costs. In order to simulate such collector as building integrated a further simulation model for the dynamic energy performance analysis of the building was also developed and validated through the prEn 15625 standard procedure. Therefore, a complete computer simulation tool (written in MatLab) was obtained by suitably merging such 2 models. Both active and passive effects of the building integrated solar collectors can be assessed in order to achieve energy, economic and environmental performance results of the whole building-solar collectors system. At last, in order to show the potentiality of the presented tool a novel case study was developed. It refers to a non-residential building with 26 solar collectors integrated in the related South-façade. The simulation analysis was carried out for different weather zones. Interesting energy, economic and CO_2 emissions savings are achieved. The presented tool and the related obtained results could be useful for new or renovated buildings designs.

7. Acknowledgments

Authors wish to acknowledge Action TU1205 (Building Integration of Solar Thermal Systems, BISTS) of the European COST (Cooperation in Science and Technology), for the sponsorship and the valuable scientific support.

8. References

Buonomano, A. and A. Palombo (2014). "Building energy performance analysis by an in-house developed dynamic simulation code: An investigation for different case studies." Applied Energy **113**: 788-807.

Duffie, J. A. and W. A. Beckman (2013). Solar engineering of thermal processes Forth Edition.

Kalogirou, S. (2014). Solar energy engineering processes and systems. Second Edition.

PrEn15625 (2007). Thermal performance of buildings – Calculation of energy use for space heating and cooling – General criteria and validation procedures.